JOURNAL OF GEOPHYSICAL RESEARCH, VOL. 88, NO. A1, PAGES 329–340, JANUARY 1, 1983

Auroral Hiss, Z Mode Radiation, and Auroral Kilometric Radiation in the Polar Magnetosphere: DE 1 Observations

D. A. GURNETT, S. D. SHAWHAN, AND R. R. SHAW

Department of Physics and Astronomy, The University of Iowa, Iowa City, Iowa 52242

The polar-orbiting DE 1 spacecraft is now providing the first measurements of high-latitude auroral phenomena in the radial distance range between about 2 and 5 R_E, where several important types of auroral plasma wave emissions are believed to be generated. This paper describes the initial observations from the DE 1 plasma wave instrument in this interesting region. Three principal types of plasma wave emissions are discussed: auroral hiss, Z mode radiation, and auroral kilometric radiation. Whistler mode auroral hiss emissions are observed on essentially every pass over the auroral zone. The auroral hiss usually has a characteristic 'funnel-shaped' frequency-time spectrum which can be explained by a simple whistler mode propagation effect if the radiation is emitted from a spatially localized source below the spacecraft. Ray path studies show that the auroral hiss is propagating upward from a source, the lower boundary of which is an altitude of about 0.7–0.9 R_E. The DE 1 observations have identified broadband Z mode emissions in the low-density region over the auroral zone and polar cap. This radiation usually has a sharply defined upper cutoff near the electron gyrofrequency and extends downward in frequency to a cutoff called the $f_{L=0}$ cutoff. The Z mode radiation is sometimes difficult to distinguish from the auroral hiss, which occurs in the same general frequency range with about the same intensity. The Z mode radiation probably corresponds to the noise previously identified as 'continuum radiation' in the Hawkeye polar region data. The auroral hiss can usually be distinguished from the Z mode radiation by the sharp upper cutoff of the whistler mode at the local electron plasma frequency. Broadband emissions identified as auroral kilometric radiation are frequently observed over the evening auroral regions at frequencies between about 100 kHz and 400 kHz. These emissions are very intense, usually 30–50 dB above the intensity of the auroral hiss and Z mode radiation, and are highly variable, sometimes disappearing completely. The auroral kilometric radiation usually occurs at frequencies above the electron gyrofrequency, consistent with earlier measurements which indicate that this radiation is propagating in the free-space R-X mode.

INTRODUCTION

For many years it has been known that intense plasma and radio wave emissions are generated in the earth's polar regions. Satellite measurements have established, for example, that intense kilometric radio emissions and whistler mode auroral hiss emissions are generated at high altitudes over the auroral regions by electrons associated with the auroral acceleration process. For a survey of the various types of plasma wave emissions observed along the auroral field lines, see the review by *Shawhan* [1979]. Up to the present time, all of the available measurements in the polar regions have been obtained either relatively close to the earth, at radial distances below about 2 R_E from low-altitude polar orbiting spacecraft, or very far from the earth, beyond about 5 R_E, as in the Heos 2 and Hawkeye investigations of the polar cusp [*D'Angelo et al.*, 1974; *Gurnett and Frank*, 1978]. This orbital coverage of the polar region leaves a gap in the important radial distance range from about 2 to 5 R_E. This radial distance range is believed to be a crucial region for the acceleration of auroral particles, and includes the region where the most intense auroral radio emissions are believed to be generated. With the launch of the DE 1 spacecraft on August 3, 1981, it is now possible for the first time to obtain in situ measurements in this important region. In this paper we describe the plasma waves detected by DE 1 at high altitudes over the polar regions, with particular emphasis on high-frequency emissions, near the electron gyrofrequency and plasma frequency.

Paper number 2A1534.
0148-0227/83/002A-1534$05.00

The orbit of DE 1 is illustrated in Figure 1, as it appeared shortly after launch. The perigee and apogee geocentric radial distances are 1.09 and 4.65 R_E, respectively. Because the latitude of perigee advances at a rate of 108° per year, this orbit will eventually provide a complete scan of all radial distances along the auroral field lines from 1.09 to 4.65 R_E. For the period involved in this initial study, from about October through December 1981, the crossings of the northern auroral L shells occurred at radial distances ranging from about 3 to 4.5 R_E. For a description of the spacecraft and the plasma wave instrumentation, see *Hoffman and Schmerling* [1981] and *Shawhan et al.* [1982]. The plasma wave instrument uses two electric dipole antennas for electric field measurements, one with a length of 9 m tip to tip oriented parallel to the spin axis and the other with a length of 200 m tip to tip oriented perpendicular to the spin axis. The spin axis is oriented perpendicular to the orbital plane. A magnetic loop antenna is also available to distinguish between electrostatic and electromagnetic waves.

Before proceeding with the description and analysis of the data, it is useful to briefly review the types of plasma wave modes that are expected at high altitudes over the polar regions and to give a summary of previous observations. As discussed by *Stix* [1962], cold plasma theory predicts the existence of four separately identifiable plasma wave modes at frequencies near the electron gyrofrequency f_g and plasma frequency f_p. These modes are the free-space L-O (left-hand polarized, ordinary) mode, the free-space R-X (right-hand polarized, extraordinary) mode, the Z mode, and the whistler mode. The Z mode is named after the so-called 'Z trace' observed on ground ionograms [*Ratcliffe*, 1959], and the whistler mode is named after the well-known lightning generated signals called whis-

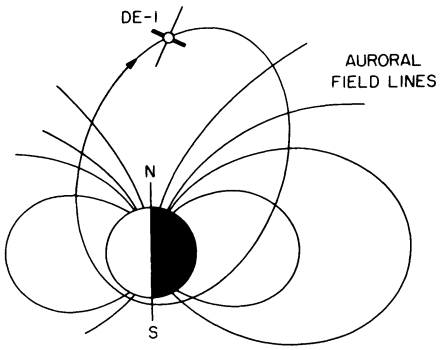

Fig. 1. A representative DE 1 orbit for the time interval analyzed in this paper. All data presented are from high-altitude passes over the northern polar region.

tlers [*Storey*, 1953]. Other modes can arise from hot plasma effects; however, for our present purposes it is sufficient to limit the discussion to the above four modes. The frequency range of these four modes is summarized in Figure 2 by using a representative model for the electron density profile over the polar region. The low-frequency cutoffs of the *L-O* and *R-X* free space modes are at the electron plasma frequency f_p and the $R = 0$ cutoff, $f_{R=0} = f_g/2 + ((f_g/2)^2 + f_p^2)^{1/2}$. The *Z* mode is bounded by the upper hybrid resonance, $f_{UHR} = (f_g^2 + f_p^2)^{1/2}$, and the $L = 0$ cutoff, $f_{L=0} = -f_g/2 + ((f_g/2)^2 + f_p^2)^{1/2}$. The whistler mode is confined to frequencies below either f_p or f_g, whichever is lower.

To varying degrees, each of the four cold plasma modes have been associated with some type of auroral plasma wave emission. At VLF frequencies both ground and satellite measurements have established the existence of a broadband electromagnetic emission called auroral hiss, which is generated in the whistler mode by low-energy (100 eV to 10 keV) auroral electrons [*Martin et al.*, 1960; *Gurnett*, 1966; *Jorgensen*, 1968; *Gurnett and Frank*, 1972; *Laaspere and Hoffman*, 1976]. Ray path studies, based on the characteristic V-shaped low-frequency cutoff of the radiation observed at low altitudes, place the source of the auroral hiss relatively high in the polar ionosphere, at altitudes from about 5000 to 10,000 km [*Gurnett and Frank*, 1972]. Upward propagating auroral hiss, usually called 'saucers,' has also been observed by low-altitude polar orbiting satellites [*Smith*, 1969; *Mosier and Gurnett*, 1969; *James*, 1976]. The source of saucer emissions is somewhat lower in the ionosphere at altitudes ranging from 1000 to 3000 km.

At higher frequencies, intense radio emissions called auroral kilometric radiation are generated in the high-latitude auroral regions in association with inverted V electron precipitation regions [*Gurnett*, 1974; *Kaiser and Stone*, 1975; *Kurth et al.*, 1975; *Green et al.*, 1979; *Benson and Calvert*, 1979]. This radiation is believed to originate at radial distances ranging from 2 to 4 R_E along the auroral field lines [*Gallagher and Gurnett*, 1979]. Because the radiation escapes freely from the earth it must be propagating in one of the two free-space modes. Several independent mode identification studies, including recent direct measurements of the polarization with DE 1 [*Shawhan and Gurnett*, 1982], provide strong evidence that the radiation is generated in the right-hand polarized *R-X* mode [*Gurnett and Green*, 1978; *Kaiser et al.*, 1978; *Benson and Calvert*, 1979]. The mode of propagation of the auroral kilometric radiation is not, however, without controversy, since *Oya and Morioka* [1982] have recently presented evidence that the radiation is generated in the left-hand polarized *L-O* mode. It is possible, of course, that the kilometric radiation may consist of both modes. However, the recent polarization measurements of *Shawhan and Gurnett* [1982] strongly indicate that the dominant component is propagating in the *R-X* mode, although some *L-O* mode may be present.

Because of the electrostatic character of the *Z* mode near the upper hybrid resonance, it has often been suggested that intense *Z* mode radiation should be produced by auroral electron beams [*Taylor and Shawhan*, 1974; *Kaufman et al.*, 1978; *Maggs and Lotko*, 1981]. Intense *Z* mode emissions have, for example, been proposed for generating auroral kilometric radiation via mode coupling with one of the free-space modes [*Benson*, 1975; *Barbosa*, 1976; *Jones*, 1977; *Roux and Pellat*, 1979; *Oya and Morioka*, 1982]. Despite the theoretical interest in *Z* mode emissions, relatively little is known about these emissions in the auroral regions. The best examples of *Z* mode emissions have been obtained in regions of relatively high plasma density in the ionosphere [*Walsh et al.*, 1964], near the equatorial plane [*Mosier et al.*, 1973; *Shaw and Gurnett*, 1975], and at low altitudes over the polar regions [*Gregory*, 1969; *Hartz*, 1969; *Muldrew*, 1970]. The ionospheric model in Figure 2 suggests that *Z* mode emissions should be quite different in the low density plasma over the polar region, where $f_p \ll f_g$ and the bandwidth of the *Z* mode is very large. Recently, *Calvert* [1981], using data from Hawkeye, has identified a type of broadband emission which he interprets as *Z* mode radiation in regions of very low density at radial distances of 2–3 R_E over the auroral zone. As will be shown, the DE 1 observations confirm this identification of *Z* mode radiation at high altitudes over the auroral zone and demonstrate that broadband *Z* mode emissions are a common feature of the polar magnetosphere.

OBSERVATIONS

Frequency-time spectrograms illustrating representative electric field spectrums obtained by DE 1 over the northern polar region are shown in Figures 3 and 4. Both spectrograms show north-to-south passes over the evening auroral zone at radial distances of about 3 R_E. These two passes have been selected for analysis because of the markedly different electron

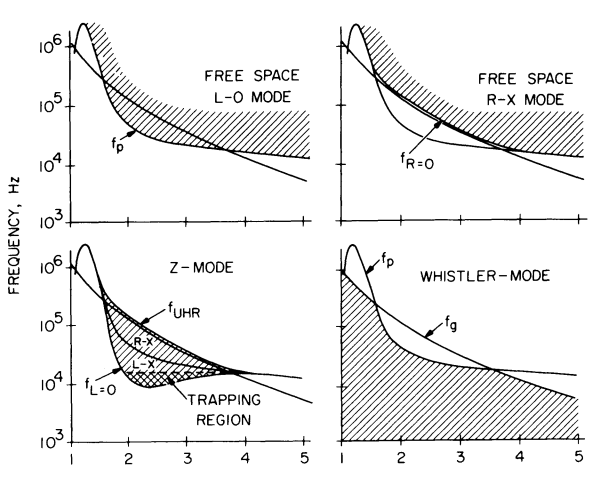

Fig. 2. The frequency range of the four high frequency cold plasma modes for a representative model of the electron density profile over the polar region. The two free-space modes can escape from the earth, whereas the whistler mode and *Z* mode are permanently trapped within the magnetosphere.

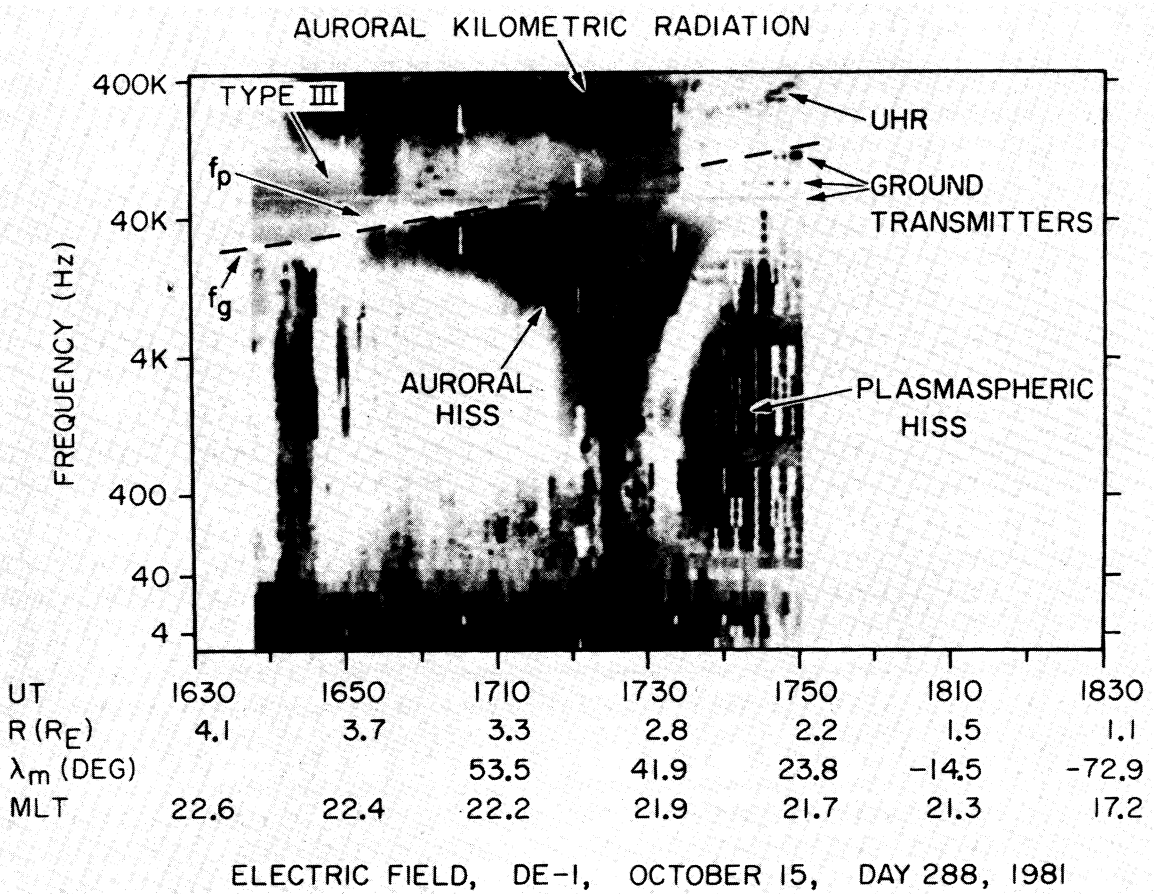

Fig. 3. A representative spectrogram of the electric field intensities for a nightside crossing of the auroral field lines. The plasma density over the polar cap in this case is relatively high, with $f_p \gtrsim f_g$.

density profiles, which strongly affect the type of plasma waves observed. To aid in the presentation, the electron gyrofrequency and plasma frequency are indicated on the spectrograms. The electron gyrofrequency, $f_g = 28B$ Hz, where B is in nanoteslas, can be calculated directly from the spacecraft magnetometer data and is therefore a determined quantity. On the other hand, the electron plasma frequency $f_p = 9(n_e)^{1/2}$ kHz, where the electron density n_e is in cm^{-3}, must be obtained by interpretation of the data.

For the event in Figure 3 the electron plasma frequency can be obtained in an unambiguous way from the low frequency cutoff of a type III solar radio burst which happened to be occurring during this pass. The type III emission corresponds to the relatively weak continuous emission evident from about 30 to 100 kHz, starting on the left side of the spectrogram. The identification of this emission as a type III solar radio burst was independently verified by measurements from the ISEE 1 spacecraft. Because the type III radio emission at low frequencies is randomly polarized and has a nearly isotropic angular distribution, the spectrum is expected to have a sharp cutoff at the local electron plasma frequency, which is the lowest cutoff frequency of the two free-space modes. The cutoff is a local effect because we expect the electron plasma frequency to increase monotonically with decreasing radial distance, thereby introducing a cutoff at the local plasma frequency for waves propagating perpendicular to the constant density contour. This cutoff is evident in Figure 3. As can be seen the electron plasma frequency is above the electron gyrofrequency over most of the polar region, from about 1638 to 1720 UT. From about 1720 to 1735 UT, it is difficult to determine the electron plasma frequency because of the superposition of several emissions in this region. After about 1735 UT the spacecraft enters the plasmasphere. In the plasmasphere the plasma frequency can be determined from narrowband upper hybrid emissions of the type discussed by *Mosier et al.* [1973]. Note that $f_g \ll f_p$ in this region, so that $f_p \simeq f_{UHR}$.

Having established the general nature of the electron plasma frequency and gyrofrequency profiles, we can now identify the mode of propagation of the primary plasma wave emissions observed during this pass. The intense 'funnel-shaped' feature centered on about 1728 UT, with an upper frequency cutoff slightly below the electron gyrofrequency, is auroral hiss. As can be seen by referring to Figure 2, this emission must be propagating in the whistler mode because the whistler mode is the only electromagnetic mode that can propagate in this frequency range. Separate magnetic field measurements, not shown, confirm that the auroral hiss is electromagnetic. As will be discussed later, the funnel shape of the frequency-time spectrum of the auroral hiss is a propagation effect caused by a frequency dependence beaming of the whistler mode radiation along the magnetic field. The basic spectral shape is quite similar to the 'V-shaped' auroral hiss observed by low-altitude satellites [*Gurnett*, 1966]. The major difference is that the funnel-shaped emissions observed by DE 1 at high altitudes propagate upward from a source below the satellite, whereas for the low-altitude observations the V-shaped events propagate downward from a source above the satellite. Comparisons with the DE 1 plasma observations (J. Burch and D. Win-

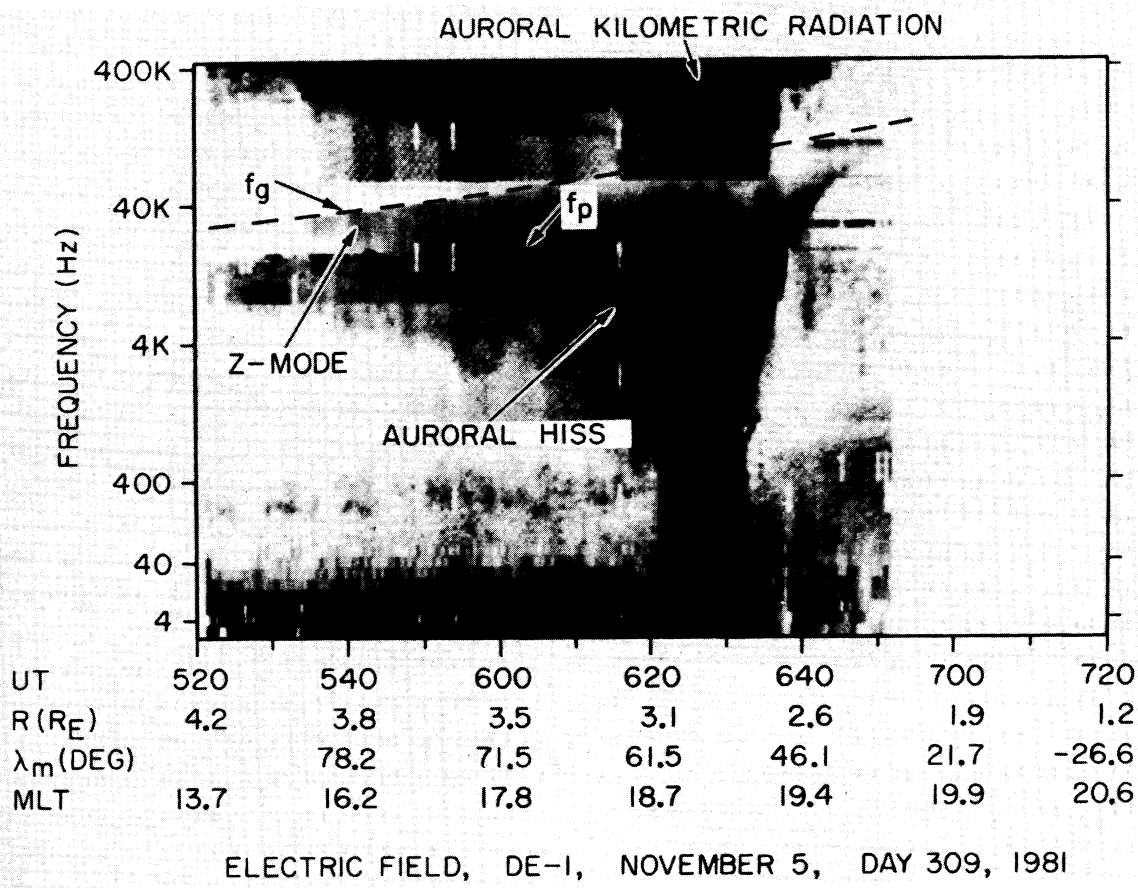

Fig. 4. Another nightside crossing of the auroral field lines, in this case selected from a period when the plasma density over the polar region is relatively low, with $f_p \ll f_g$.

ningham, personal communication, 1981) confirm that the vertex of the funnel at about 1728 UT in Figure 3 is centered on a region of intense auroral electron precipitation.

At frequencies above the electron plasma frequency an intense band of radiation can be seen in Figure 3 from about 100 to 400 kHz. On the basis of comparisons with similar observations from other spacecraft, this radiation is identified as auroral kilometric radiation. Separate magnetic field measurements, not shown, confirm that this radiation is electromagnetic and that the polarization is right hand with respect to the magnetic field, as expected for the free-space *R-X* mode. Because the electric field intensities are very large, 1–10 mV/m, some of the features extending downward from the main emission band are spurious effects caused by saturation of the receiver. These features terminate abruptly at 50 kHz, which corresponds to a transition between two adjacent frequency ranges in the receiver. The spurious character of these features has been confirmed by comparisons with measurements from the shorter, 9 m tip to tip, spin axis antenna which does not display these saturation effects. Other features evident in Figure 3 include whistler mode signals from ground VLF transmitters and whistler mode plasmaspheric hiss. It is interesting to note that the high-latitude, high-frequency cutoff of the plasmaspheric hiss has a frequency dependence almost identical to the low-latitude, low-frequency cutoff of the auroral hiss.

For the second pass selected for discussion, in Figure 4, the electron plasma frequency is well below the electron gyrofrequency. The electron plasma frequency in this case can be identified from the very sharp upper frequency cutoff of the auroral hiss. As shown in Figure 2, when $f_p < f_g$ the upper cutoff of the whistler mode is at the electron plasma frequency. In this case, upward propagating auroral hiss emissions are expected to show a sharp cutoff at f_p, exactly as is observed. Above the plasma frequency another band of emission can be seen with a sharp upper frequency cutoff at the electron gyrofrequency. This band can be identified most clearly over the polar cap, from about 0540 to 0620 UT, and becomes more difficult to distinguish from the auroral hiss emissions over the auroral zone, from about 0620 to 0640 UT. Magnetic field measurements show that this band has a magnetic field component and therefore consists of electromagnetic radiation. Comparisons with Figure 2 show that this emission must be propagating in the *Z* mode, because the free-space *L-O* mode, which is the only other electromagnetic mode that can propagate in the frequency range $f_p < f < f_g$, has no cutoff or resonance effect at the electron gyrofrequency. As indicated in the shaded region in Figure 2, when $f_p \ll f_g$ the *Z* mode bandwidth becomes very broad, extending from approximately f_p^2/f_g to f_g. Under these conditions the *Z* mode overlaps considerably with the whistler mode, thereby making it difficult to distinguish the *Z* mode radiation from auroral hiss. The *Z* mode also overlaps with the free-space *L-O* mode, and only a very small gap exists between the *Z* mode and the free-space *R-X* mode, thus making it difficult to distinguish *Z* mode radiation from the kilometric radio emissions.

In retrospect, the existence of *Z* mode emissions between f_p and f_g explains why the noise identified as 'auroral hiss' in the Hawkeye data [*Gurnett and Green*, 1978] sometimes appeared to extend continuously up into the auroral kilometric radiation spectrum. In some cases the 'auroral hiss' in the Hawkeye data may have consisted of superposed *Z* mode and whistler mode radiation. *Calvert* [1981] has previously pointed out this in-

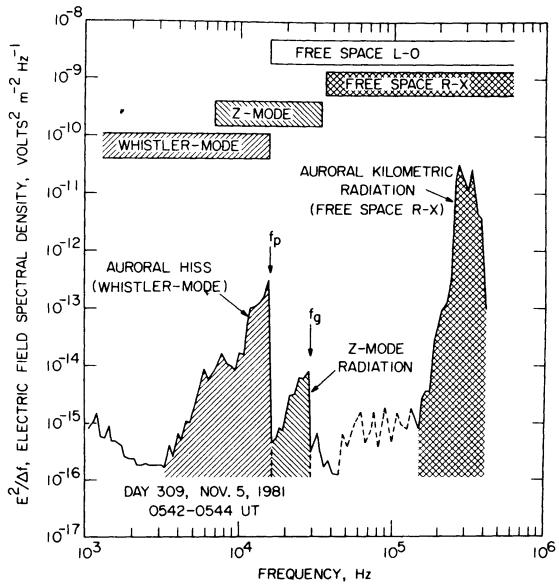

Fig. 5. An electric field intensity spectrum selected from the pass in Figure 4 showing the relative intensities of the auroral kilometric radiation, the Z mode radiation, and the auroral hiss. The sharp upper cutoff of the auroral hiss at f_p and the cutoff of the Z mode radiation at f_g are clearly evident. The dashed line indicates a region where the spectrum is being modified by receiver distortion effects caused by the very intense kilometric radiation.

terpretation of the Hawkeye data. Also, the radiation identified as continuum radiation in the Hawkeye data was probably Z mode radiation. As discussed by *Gurnett and Green* [1978], the noise identified as continuum radiation usually extended over most of the polar region at frequencies slightly below the electron cyclotron frequency. The noise had very smooth temporal variations with intensities of about 1.3×10^{-17} W m^{-2} Hz^{-1} (4.9×10^{-15} V m^{-2} Hz^{-1}). These characteristics are almost identical to the emissions now identified as Z mode radiation in the DE 1 data. The identifying feature of Z mode radiation, which is the sharp upper cutoff at $f_{UHR} \simeq f_g$, could not be identified in the Hawkeye data because of the very low intensities and the poor frequency resolution. The improved sensitivity and frequency resolution available with the DE 1 instrument now allows us to unambiguously resolve these different emissions to an extent that simply was not possible with the 16-channel spectrum analyzer on Hawkeye. Radiation comparable to the trapped continuum radiation detected by *Gurnett and Shaw* [1973] near the equatorial plane has not yet been identified in the DE 1 data over the polar regions. The trapped continuum radiation is a relatively weak emission (average intensity 1.0×10^{-15} V^2 m^{-2} Hz^{-1} at 10 kHz) that usually reaches maximum intensity below 10 kHz. This radiation, if it exists over the polar region, is most likely being masked by the more intense Z mode and auroral hiss emissions.

The relative intensity of the three different types of radiation identified in Figure 4 is illustrated in Figure 5. The dashed part of the spectrum indicates the frequency range where receiver saturation problems are being caused by the intense auroral kilometric radiation. The actual spectral density in this frequency range is below the dashed line, and the abrupt decrease at 50 kHz is caused by the transition to the next lower frequency band, which is not affected by the saturation effects in the highest frequency band. The sharp cutoffs in the frequency spectrum at the electron plasma frequency and gyrofrequency are clearly evident. The bar labeled 'Z mode' near the top of the plot shows the low-frequency cutoff, $f_{L=0}$, of the Z mode computed from f_p and f_g. No intensity change is evident at $f_{L=0}$, probably because the auroral hiss masks any Z mode radiation which may be extending down into this part of the frequency spectrum. Occasionally, when the auroral hiss intensity is sufficiently low, the Z mode radiation can be seen extending down to $f_{L=0}$. One such case is illustrated in Figure 6, which shows a

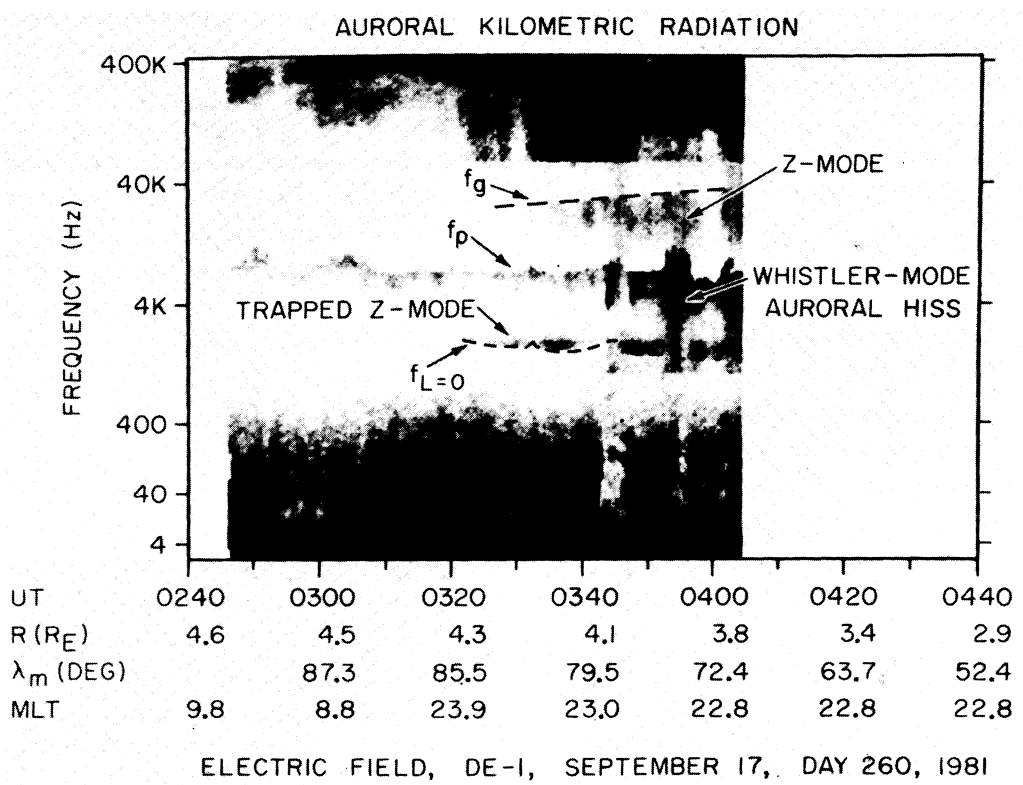

Fig. 6. One of the few cases where the low-frequency cutoff of the Z mode at $f_{L=0}$ can be identified. This example may represent a case in which Z mode radiation is trapped in a cavity formed by a local minimum in $f_{L=0}$.

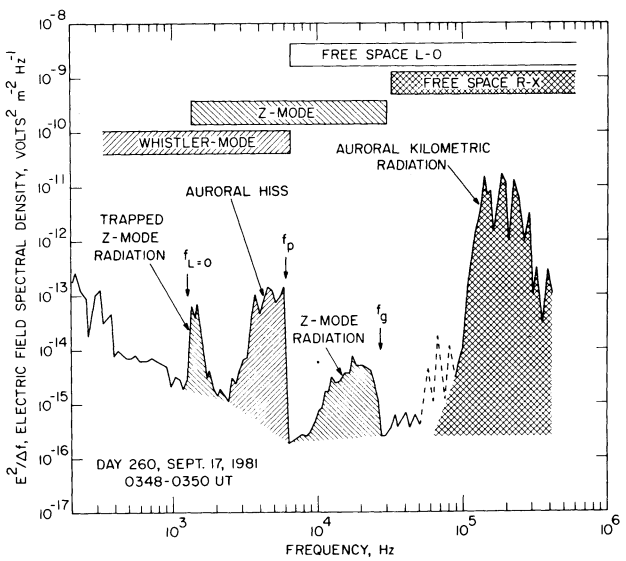

Fig. 7. An electric field intensity spectrum selected from the pass in Figure 6 showing the close agreement between the computed $f_{L=0}$ cutoff (bar labeled Z mode) and the low frequency cutoff of the band identified as trapped Z mode radiation.

band of enhanced electric field intensities just above the computed low-frequency cutoff $f_{L=0}$ of the Z mode. Because this band has a well-defined upper cutoff which remains constant throughout the entire pass, it is our tentative conclusion that this band represents a range of frequencies in which the Z mode can be trapped within the ionosphere near a local minimum in $f_{L=0}$. This region of trapped Z mode radiation is indicated by the double cross-hatching in Figure 2. Once trapped in the cavity formed by a local minimum in $f_{L=0}$ the radiation should be subject to very little attenuation or loss and could build up to large intensities. A spectrum illustrating the relative intensity of the various types of radiation identified in Figure 6 is shown in Figure 7. The computed low-frequency cutoff of the Z mode is seen to be in good agreement with the low-frequency cutoff of the band identified as trapped Z mode radiation.

Further details of the upper cutoff of the auroral hiss are illustrated in Figure 8, which shows a high-resolution wideband spectrogram of an auroral hiss event similar to the events in Figures 3 and 4. Evidence for the close proximity of the upper cutoff of the auroral hiss to the local electron plasma frequency is given in this case by the occurrence of an intense narrowband emission slightly above the upper cutoff of the auroral hiss from about 1417:42 to 1418:00 UT. The frequency of this emission is well below the electron gyrofrequency, which is about 24.6 kHz at this time. Because of the frequency, $f < f_g$, and the close proximity to the upper cutoff of the aurora hiss, which is expected to be near f_p, it is our interpretation that this narrowband emission is an electron plasma oscillation at the local electron plasma frequency f_p. The phase of the spin modulation, with nulls at about 1417:52 and 1417:55 UT, indicates that the electric field of this emission is aligned very nearly parallel to the static magnetic field, which is the expected orientation for an electron plasma oscillations driven by a field-aligned electron beam. If the emission is an electron plasma oscillation, this observation shows that the upper cutoff of the auroral hiss is very close to the local electron plasma frequency ($\sim$5–10% below). Narrowband electron plasma oscillations, near and slightly above the upper cutoff of the auroral hiss, are a common feature of the DE 1 observation over the polar region whenever $f_p < f_g$. When $f_p > f_g$, another type of narrowband electrostatic emission somewhat similar in appearance to that shown in Figure 8 occurs slightly above the electron gyrofrequency. An example of this type of emission is illustrated in Figure 9, which shows a pass through the polar cusp near local noon. These emissions are identified as $3f_g/2$ emissions or, more generally, electron cyclotron emissions [*Kennel et al.*, 1970]. Electron cyclotron emissions of this type are frequently observed in the vicinity of the dayside polar cusp and are probably of the same type observed by *Gurnett and Frank* [1978] at somewhat higher altitudes in the polar cusp by using Hawkeye data.

AURORAL HISS PROPAGATION AND SOURCE

As mentioned in the previous section, the funnel-shaped appearance of the auroral hiss spectrum has a simple interpretation based on the propagation of whistler mode waves from a spatially localized source. For several years it has been believed that auroral hiss is propagating at wave normal angles very close to the resonance cone, in a regime where the whistler mode is quasi-electrostatic [*Smith*, 1969; *Mosier and Gurnett*, 1969; *Gurnett and Frank*, 1972; *James*, 1976]. For wave normal angles near the resonance cone it can be shown that the ray path direction is perpendicular to the resonance cone at an angle ψ_{res} with respect to the magnetic field, as shown in Figure 10. The angle ψ_{res} is given by

$$\tan^2 \psi_{res} = -\frac{S}{P} \simeq \frac{f^2 f_p^2}{(f_p^2 - f^2)(f_g^2 - f^2)} \tag{1}$$

where S and P are defined by Stix [1962], and the approximation assumes that the frequency is sufficiently high for ion effects to be negligible and for S to be much greater than 1 (high-density approximation).

Equation (1) shows that at low frequencies ($f \rightarrow 0$) the ray path is almost exactly along the magnetic field ($\psi_{res} \rightarrow 0$). As the frequency increases, the ray path angle relative to the magnetic field increases, becoming perpendicular ($\psi_{res} \rightarrow \pi/2$) when f reaches either f_p or f_g, whichever is lower. Because the plasma frequency and gyrofrequency decrease with increasing altitude, the effect on an upward propagating wave is for the ray path to start out along the magnetic field and then deviate increasingly from the magnetic field direction, approaching perpendicular as f approaches $\min\{f_p, f_g\}$. The qualitative form of the ray paths for a point source emitting waves upward along a vertical magnetic field is shown in Figure 10. Because of the frequency dependence in equation (1), low frequencies are beamed nearly parallel to the magnetic field, and higher frequencies are beamed at progressively larger angles to the magnetic field. If a satellite passes horizontally through this beam of radiation the highest frequencies are detected first, and the frequency decreases monotonically as the satellite approaches the source. The minimum frequency occurs as the satellite crosses the magnetic field line through the source.

The detailed shape of the radiation spectrum within the beam is determined by the source geometry. For a point source, the radiation propagates upward in a thin conical pattern which is rotationally symmetric around the magnetic field. The frequency-time spectrogram in this case would consist of a single emission line, the center frequency of which is controlled by the frequency dependence of the beam width, as in Figure 10. If the source is an extended horizontal line, the radiation spectrum can be thought of as a superposition of conical emis-

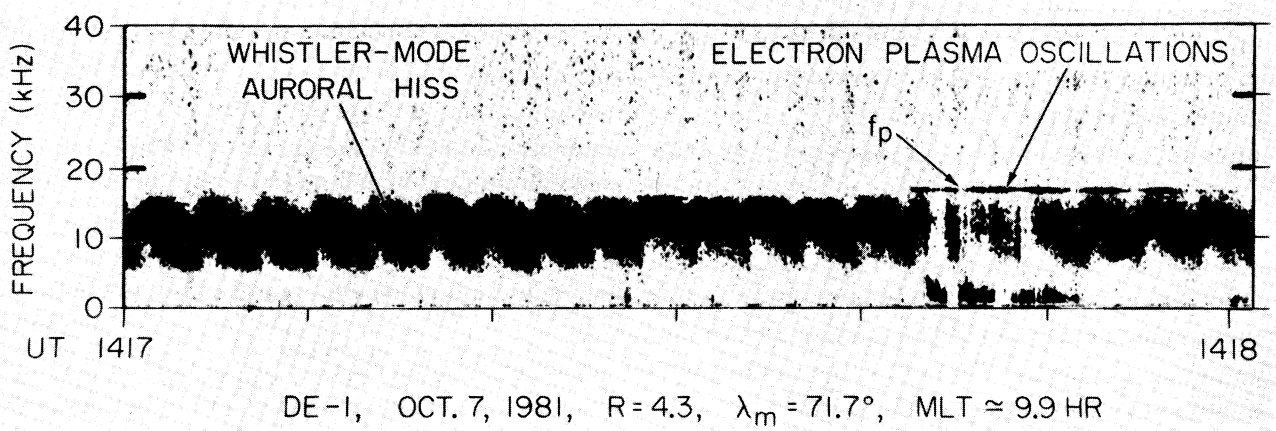

Fig. 8. A high-resolution frequency-time spectrogram of the upper cutoff of the auroral hiss. The narrowband emission is believed to be an electron plasma oscillation at the local electron plasma frequency f_p.

sion patterns from a series of point sources uniformly distributed along the line. Because the auroral hiss detected by DE 1 almost always fills the entire region within the funnel, the emission must be generated over an extended region. The existence of a sharply defined frequency-time boundary to the funnel indicates that the source has a sharply defined low-altitude boundary, corresponding to either a horizontal line source oriented roughly in an east-west direction, or a field-aligned sheet source with a sharp low-altitude boundary.

To perform a quantitative test of this whistler mode propagation model a series of ray tracing computations have been performed to compare the computed ray path boundaries with the observed frequency-time profile of a funnel-shaped auroral hiss event. One of our objectives in these comparisons is to estimate the low-altitude boundary of the source region. To reduce the sensitivity of the ray tracing results to variations in the electron density profile, it is best to choose an event with a large plasma frequency, because then the ray path is nearly independent of the plasma density (see equation (1)). For this reason we have selected the event in Figure 3, because in this case f_p is well above f_g for most of the event.

Figure 11 shows a series of representative ray paths for a

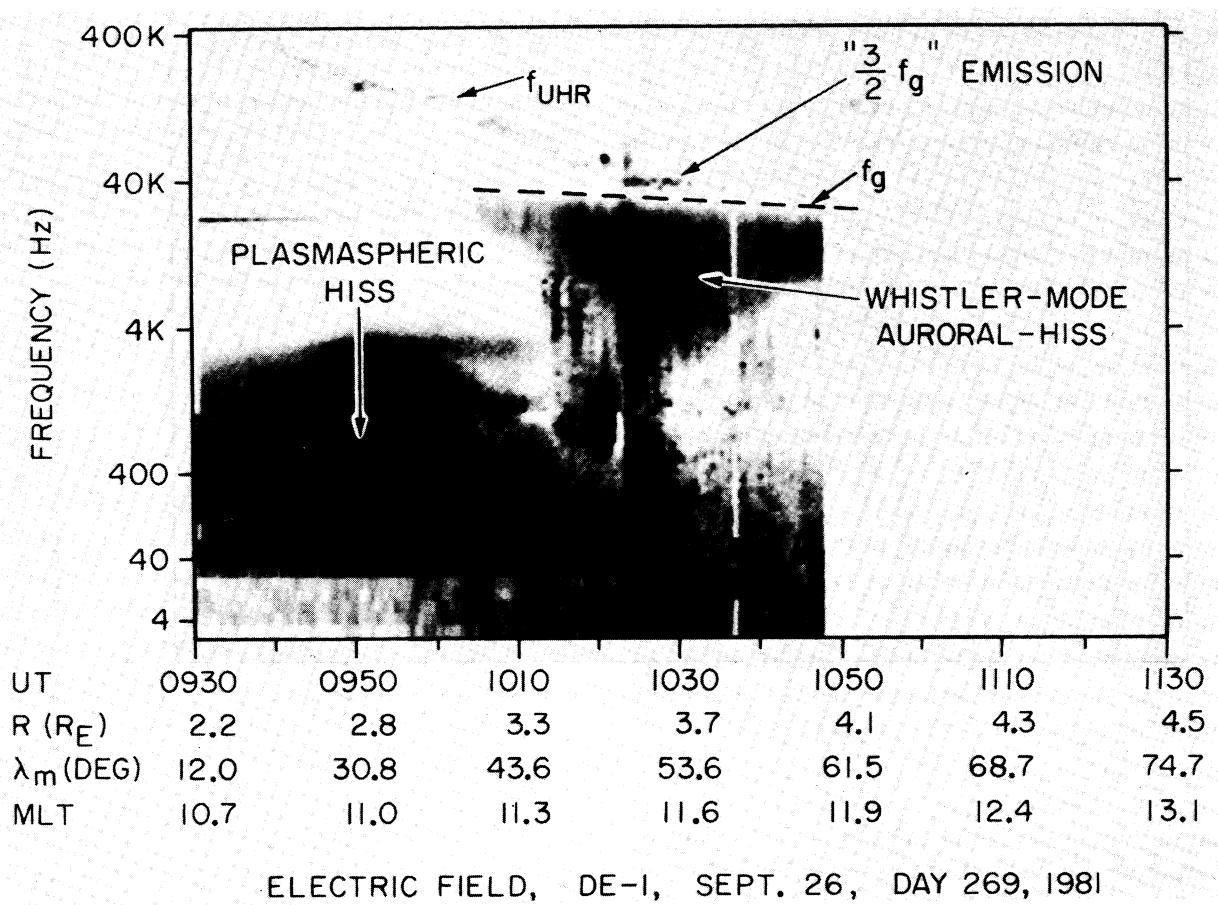

Fig. 9. A dayside pass through the auroral zone showing a funnel-shaped auroral hiss event and $3f_g/2$ electrostatic emissions associated with the polar cusp.

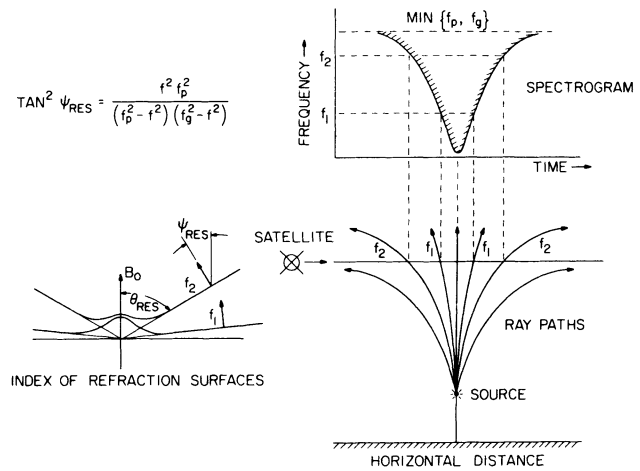

Fig. 10. The geometric constructions used to analyze the ray path of auroral hiss. For wave normal angles near the resonance cone, whistler mode emissions from a point source produce a funnel-shaped spectrum qualitatively similar to the funnel-shaped auroral hiss events observed by DE 1.

source location which provides a good fit to the auroral hiss event in Figure 3. From the times at which ray paths for various frequencies cross the spacecraft trajectory, the frequency-time boundaries of the emission can be computed. These boundaries are shown by the solid lines in Figure 12 for a series of source altitudes. Because the emission in this case appeared to extend over a finite range of L values, the source was assumed to be of finite north-south thickness and the low and high latitude boundaries of the source were adjusted until a good fit was obtained. The best fit radial distance of the low-altitude boundary of the source is about 1.7–1.9 R_E, and the low and high latitude boundaries of the source are about $L = 5.36$ and $L = 6.05$. As can be seen from Figure 12, the ray tracing fit to the observed spectrum is quite good, which provides strong evidence that the whistler mode radiation is propagating at angles very close to the resonance cone, as has been assumed. The low-altitude boundary of the source is also determined with good accuracy. Radial distances less than about 1.7 R_E are too low and greater than about 1.9 R_E are too high.

Because the auroral hiss is propagating as a quasi-electrostatic wave near the whistler mode resonance cone, it is believed that the emission is produced by a plasma instability associated with the Landau resonance at $v_{\|} = \omega/k_{\|}$, and not the cyclotron resonance at $v_{\|} = (\omega_g - \omega)/k_{\|}$ [*James*, 1976; *Maggs*, 1976]. Because the Landau resonance (which is the same resonance involved in the incoherent Cerenkov mechanisms) involves interactions with particles traveling in the same direction as the wave, the upward propagating auroral hiss detected at high altitudes by DE 1 must be produced by an upgoing particle beam. Because the downgoing auroral hiss events observed at low altitudes are closely correlated with low-energy (100 eV to 10 keV), inverted V electron precipitation, it seems likely that the auroral hiss observed by DE 1 is produced by an upgoing beam of low-energy electrons. At the present time we have not clearly identified the particles producing the upgoing auroral hiss, although preliminary comparisons with the charged particle measurements on DE 1 (J. Burch, D. Winningham, and E. Shelley, personal communication, 1982) show that the auroral hiss occurs in or very near regions of intense low-energy electron and ion fluxes. The sharp low-altitude boundary of the upgoing auroral hiss source at a radial distance of about 1.7–1.9 R_E strongly suggests that the upgoing particles producing the radiation have a similar altitudinal structure, possibly indicative of the region in which the particles are being accelerated.

Z Mode Propagation and Source

As can be seen from Figure 2, the bandwidth of the Z mode is a very sensitive function of the plasma frequency to gyrofrequency ratio. When f_p/f_g is much greater than 1 the bandwidth is very narrow, whereas when f_p/f_g is much less than 1 the bandwidth is very broad. Narrowband Z mode emissions, often referred to as UHR emissions, have been extensively studied in regions of relatively high density ($f_p \gtrsim f_g$) near the equatorial plane by low-latitude, eccentric-orbiting spacecraft. Because of the broad frequency range of the Z mode in the low densities over the polar region, these emissions can propagate over relatively large distances, both horizontally and vertically. This situation is in sharp contrast to the narrowband equatorial Z mode emissions, which are frequently considered to be a 'local' emission because of the narrow altitude band in which the radiation can propagate. An analysis of the propagation of the Z mode over the polar regions is somewhat complicated and is best performed by computer tracing techniques such as those performed by *Jones* [1977] and *James* [1978]. The general nature of the Z mode propagation can, however, be understood by considering the various shapes the index of refraction surface can have in different regions of the CMA diagram [*Ratcliffe*, 1959; *Budden*, 1961; *Stix*, 1962]. The shape of the index of refraction surface is indicated schematically in Figure 13 for a sequence of altitudes ranging from the low-frequency cutoff at $f_{L=0}$ to the high-frequency limit at f_{UHR}. The topology of the index of refraction surface changes at the gyrofrequency. Above the gyrofrequency the index of refraction surface has a resonance cone, with no propagation allowed for wave normal angles from 0 to θ_{res}. Below the gyrofrequency, propagation is allowed for all wave normal angles, with the index of refraction surface taking on a more-or-less elliptical shape, ranging from an elongated cigar-shaped surface of revolution slightly below f_g to a slightly oblate spheroid near $f_{L=0}$. The index of refrac-

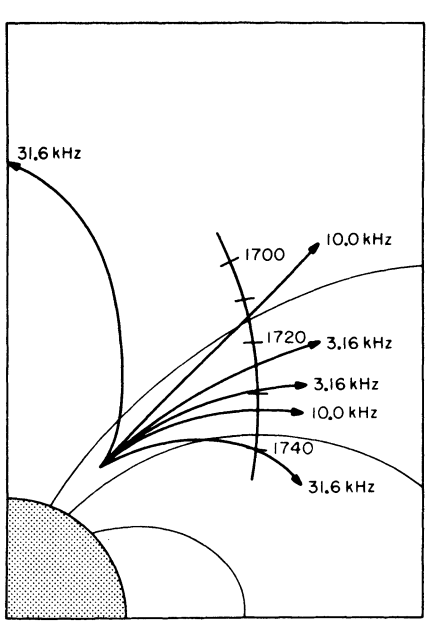

Fig. 11. A series of whistler mode ray paths computed for a source position which produces a good fit to the funnel-shaped auroral hiss event in Figure 3.

tion goes to zero for all angles at $f_{L=0}$. Upon crossing the gyrofrequency the index of refraction surface transforms smoothly from an elongated cigar-shaped surface below the gyrofrequency to a resonance cone type of surface above the gyrofrequency. At the plasma frequency the index of refraction undergoes a complicated change in shape near $\theta = 0$, forming a dimple as the frequency approaches f_p from below, degenerating to a line at f_p, and changing to a nipple above f_p [see *Budden*, 1961]. The labeling of the Z mode also changes at the plasma frequency, from L-X below f_p to R-X above f_p (see Figure 2).

To gain a qualitative understanding of the Z mode propagation in the low-density regime encountered by DE 1 over the polar region, we make use of a simple construction introduced by *Poeverlein* [1949]. If we assume for simplicity that the medium is horizontally stratified with the magnetic field vertical, as it would be over the polar regions, Snell's law shows that the horizontal component of the index of refraction vector is constant. In Figure 13 the conservation of the horizontal component of the index of refraction can be imposed by requiring that the index of refraction vector fall on a vertical dashed line drawn through the index of refraction surfaces. The ray path direction is then given by the normal to the index of refraction surface at the intersection with the dashed line. From the above construction it is evident that a wave originating in the region below f_g cannot in general reach the region above f_g, and vice versa. If a wave is launched downward from a source below f_g, the wave tends to refract upward because the index of refraction goes to zero at the $f_{L=0}$ cutoff. The wave always reflects at some point before reaching $f_{L=0}$, as shown in Figure 13, except for the special case of vertical incidence. After reflection the wave propagates upward with relatively little refraction until it approaches the level where $f = f_g$. In this region the ray path starts to bend horizontally, asymptotically approaching f_g from below. This tendency toward horizontal propagation is caused by the elongation of the cigar-shaped index of refraction surface as the wave frequency approaches f_g from below.

For magnetic field directions tilted away from vertical the qualitative behavior of the ray paths is essentially the same as in Figure 13, except that waves incident from below can under some circumstances propagate into the region above f_g. The entry into the region above f_g, however, remains restricted to

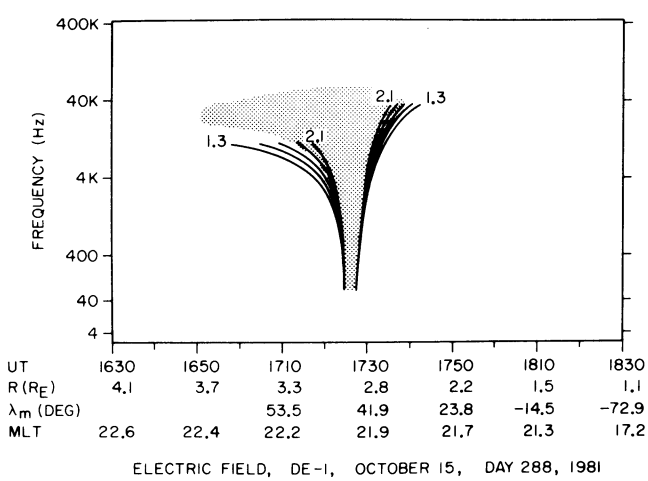

Fig. 12. The frequency-time boundaries computed from ray paths similar to those in Figure 10, for a range of source radial distances for the event in Figure 3 (shaded area). The best fit source position is at a radial distance between 1.7 and 1.9 R_E.

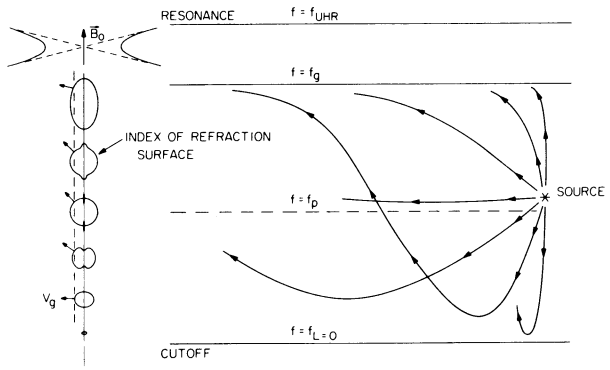

Fig. 13. The geometric constructions used to analyze the ray path of Z mode radiation. The Z mode radiation can propagate large distances horizontally and has a tendency to be refracted asymptotically to the level slightly below $f = f_g$.

the region near $f = f_g$ for magnetic field directions near vertical. Also, for wave normal angles near $\theta = 0$ the dimple and nipple which form in the index of refraction surface near $f = f_p$ (see Figure 13) can cause some unusual ray path characteristics in this region, including 'spitze' reflections of the type discussed by *Budden* [1961]. However, except for a very restricted range of wave normal angles near vertical, these unusual ray path geometries are probably not important for the Z mode radiation detected by DE 1 over the polar region.

The simple ray path considerations illustrated in Figure 13 account for most of the primary characteristics of the Z mode radiation detected by DE 1. The ability of the radiation to propagate horizontally with relatively little refraction (similar to free space), except near $f_{L=0}$ and f_g, explains why the radiation can be detected over a large region of the polar cap far away from the auroral region, which is the most likely source. At lower altitudes the existence of such long-range propagation has been previously demonstrated by bistatic propagation experiments with ISIS 1 and 2 [*James*, 1978, 1979], in which radio signals were transmitted several hundred kilometers horizontally across the polar cap in the Z mode. The horizontal refraction of the radiation just below f_g, and the limited accessibility to the region above f_g, explains why the radiation is usually not observed above f_g even though the Z mode extends up to f_{UHR}. The tendency of the waves to refract away from the cutoff at $f_{L=0}$ explains why the spectrum usually does not extend down to $f_{L=0}$. The fact that the radiation usually does not extend down to $f_{L=0}$ suggests that the radiation tends to be propagating with wave vectors nearly horizontal, perpendicular to **B** rather than vertical. This wave vector orientation is consistent with the large horizontal region over which the radiation can be detected and has been confirmed by investigation of the spin modulation, which tends to show maximum electric field intensities when the antenna is aligned near vertical. The only exception appears to be the case of trapped Z mode radiation, for which a nearly isotropic wave number distribution is expected because the radiation is essentially trapped in a cavity.

In considering the possible source of the Z mode radiation, there is very little direct evidence from DE 1 indicating exactly where the radiation is generated. Sometimes the bandwidth and intensity of the radiation increases as the spacecraft approaches the auroral zone as in Figure 4, which suggests an auroral source. However, no marked local intensification is usually evident in the auroral regions which could convincingly identify the auroral zone as the source. Sometimes isolated 'bursts' of Z mode emission occur over the polar region, well away from

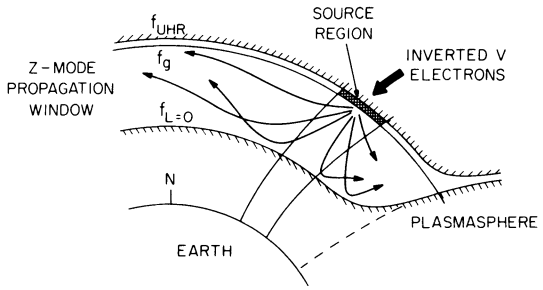

Fig. 14. The source geometry and ray paths that would occur if the Z mode radiation is generated in the frequency range between f_g and f_{UHR}, where the Z mode is quasi-electrostatic and can interact with low-energy, inverted V electrons.

the auroral zone. These isolated events could, of course, be caused by time variations in the source or changing propagation conditions between the source and the spacecraft, and do not rule out an auroral zone source. No obvious relationship is evident between the intensity of the Z mode radiation and the intensity of the auroral hiss or kilometric radiation. Of the two, the intensity variations of the Z mode radiation appear to be most similar to the auroral hiss. Both types of emissions tend to have similar intensities (within 10–20 dB) and are relatively steady, with little change on consecutive passes over the auroral zone. In contrast, the auroral kilometric radiation intensity often changes by 60–80 dB on time scales of only a few minutes and is much more variable than the Z mode radiation. In summary, it seems most likely that the Z mode radiation is generated in the same general region as the auroral hiss, but at the present time there is little hard evidence to confirm this hypothesis.

Because the Z mode becomes quasi-electrostatic and has very low phase velocities for frequencies between f_g and f_{UHR}, all current theories have concentrated on this frequency range for explaining Z mode radiation. Two general types of emission processes have been considered: incoherent Cerenkov radiation [*Taylor and Shawhan*, 1974; *Jones*, 1976] and coherent plasma instabilities [*Kaufman et al.*, 1978; *Maggs and Lotko*, 1981]. Of the plasma instabilities which have been considered, the Landau resonance at $v_{\|} = \omega/k_{\|}$ is most frequently considered, because this instability can be driven by a region of positive slope in the electron distribution function, $\partial F_e(v_{\|})/\partial v_{\|} > 0$, as would be expected in a beam of auroral electrons. In this respect the mechanisms proposed for explaining Z mode emissions are nearly identical to those proposed for explaining auroral hiss. The only difference is the mode of propagation, and even here the similarities are very close because both modes of propagation are quasi-electrostatic with wave normal angles very close to the resonance cone.

If the radiation is generated in the frequency range between f_g and f_{UHR}, an obvious question arises as to how the waves can reach the region below f_g, which is where they are observed by DE 1. Although the propagation model in Figure 13 indicates that these two regions are inaccessible, this situation occurs only when the electron density gradients are parallel to the magnetic field. When the electron density gradients are perpendicular to the magnetic field, as is expected in the field-aligned structures associated with the auroral zone, the Z mode can propagate smoothly across the level where $f = f_g$ with essentially no attenuation. In this situation a quasi-electrostatic Z mode emission generated by the electron beam above f_g can be converted directly to nearly pure electromagnetic Z mode radiation below f_g. This source geometry is illustrated in Figure 14.

If the above conversion of electron beam energy to Z mode radiation is occurring in the auroral zone, it should be possible to confirm this process with the DE 1 data. However, given the long range of propagation of the Z mode over the polar regions, it is not entirely clear how the generation mechanism can be clearly identified. One approach which has been investigated is to search for strongly enhanced emissions near the upper hybrid resonance frequency in the auroral zone. If the radiation is generated as a quasi-electrostatic emission near f_{UHR}, this emission should be strongly intensified in the vicinity of the upper hybrid resonance because of the slow group velocity in this region. At present the only intense electrostatic emission that has been detected in this frequency range is the $3f_g/2$ electrostatic emission of the type shown in Figure 9. These emissions often occur at frequencies just above f_g, in the vicinity of the upper hybrid resonance. Unfortunately, these emissions appear to be most common when $f_p \gtrsim f_g$, as in Figure 9, and have not yet been found in the low-density regions where the broadband Z mode radiation is observed. The search for electrostatic emissions associated with the Z mode is further complicated by the fact that in the auroral zone the auroral kilometric radiation often becomes so intense that receiver distortion effects tend to obscure the spectrum in the vicinity of f_{UHR}, thereby making it difficult to identify features that might be associated with the relatively weak Z mode radiation.

SUMMARY AND CONCLUSIONS

With the DE 1 plasma wave measurements we have now been able to distinguish clearly three important types of plasma wave emissions in the polar magnetosphere: auroral kilometric radiation, auroral hiss, and Z mode radiation. All three types of radiation are believed to be generated along the auroral field lines in the same general radial distance range, from about 2 to 4 R_E. The auroral kilometric radiation is observed at frequencies above the local R-X cutoff frequency, in a frequency range consistent with propagation in the right-hand polarized free space R-X mode. The kilometric radiation is by far the most intense of these three types of high-frequency radio emissions and often has broadband electric field intensities ranging from 1 to 10 mV/m.

The auroral hiss is always observed at frequencies below the auroral kilometric radiation, below either the electron gyrofrequency or the electron plasma frequency, whichever is lower. Typical broadband electric field strengths for the auroral hiss are about 30–300 μV/m. The auroral hiss usually has a distinctive funnel-shaped frequency-time spectrum which can be explained by propagation in the whistler mode at wave normal angles near the resonance cone. The auroral hiss is propagating upward from a source below the spacecraft. Ray tracing comparisons indicate that the source is either an extended horizontal line source at a radial distance of about 2 R_E, or else an extended field-aligned sheet source with a sharp lower boundary at about 2 R_E. The similarity of the DE 1 observations of upward propagating auroral hiss to observations of downward propagating auroral hiss by low-altitude satellites suggests that the radiation is probably produced by low energy electrons in the energy range from $\sim$100 eV to 10 keV. If the auroral hiss is produced by the Landau resonance, these electrons must be streaming up the magnetic field line from an acceleration region at lower altitudes. The sharp localization of the lower boundary of the auroral hiss source at a radial distance of about 2 R_E suggests that the electron acceleration may be occurring in this altitude range.

The DE 1 observations have identified broadband Z mode radiation propagating in regions of low plasma density over the auroral zones and polar cap. These observations are similar in many respects to the Z mode emissions detected at lower altitudes by the Ariel III, Alouette, and ISIS satellites [*Gregory*, 1969; *Hartz*, 1969; *Muldrew*, 1970] and the more recent Hawkeye observations of *Calvert* [1981]. The Z mode radiation occurs in the same general frequency range and with about the same intensity as the auroral hiss and probably corresponds to the 'continuum radiation' previously detected over the polar region with the Hawkeye spacecraft. The upper frequency limit of the Z mode emissions is at or very near the electron gyrofrequency. The low-frequency limit of the Z mode is at the left-hand cutoff $f_{L=0}$, which is well below the electron gyrofrequency when $f_p \ll f_g$. The Z mode radiation is usually most intense near and slightly below the electron gyrofrequency and is seldom seen extending all the way down to the cutoff at $f_{L=0}$. The low frequency cutoff of the Z mode radiation is often masked by auroral hiss emissions that occur in the same frequency range. Other theoretical investigations suggest that the Z mode radiation is probably produced by a Landau resonance with streams of low-energy auroral electrons, very similar to the generation of auroral hiss. This resonance occurs at frequencies between the electron gyrofrequency and the upper hybrid resonance in a frequency range where the Z mode is quasi-electrostatic. If suitable density gradients are present the quasi-electrostatic Z mode emissions can propagate freely into the region below the electron gyrofrequency, where the Z mode is almost purely electromagnetic.

These initial results from the DE 1 spacecraft demonstrate the many interesting radio emission processes that are occurring at high altitudes over the polar regions and the new capabilities now available to investigate these processes. As more data become available, we plan to proceed with further investigations of the origin of these wave emissions by using the extensive plasma diagnostic capabilities available on the DE spacecraft.

Acknowledgments. The authors would like to extend their thanks to R. Huff and T. Averkamp, who provided valuable assistance in the data processing. This research was supported by NASA through contract NAS5-25690 with Goddard Space Flight Center, through grants NGL-16-001-002 and NGL-16-001-043 from NASA Headquarters, and by the Office of Naval Research.

The editor thanks R. F. Benson and Dyfrig Jones for their assistance in evaluating this paper.

REFERENCES

Barbosa, D. D., Electrostatic mode coupling at f_{UHR}: A generation mechanism for auroral kilometric radiation, Ph. D. dissertation, Dept. of Phys., Univ. of Calif., Los Angeles, 1976.

Benson, R. F., Source mechanisms for terrestrial kilometric radiation, *Geophys. Res. Lett.*, *2*, 52, 1975.

Benson, R., and W. Calvert, ISIS 1 observations at the source of auroral kilometric radiation, *Geophys. Res. Lett.*, *6*, 479, 1979.

Budden, K. G., *Radio Waves in the Ionosphere*, Cambridge University Press, New York, 1961.

Calvert, W., The auroral plasma cavity, *Geophys. Res. Lett.*, *8*, 919, 1981.

D'Angelo, N., A. Bahnsen, and H. Rosenbauer, Wave and particle measurements at the polar cusp, *J. Geophys. Res.*, *79*, 3129, 1974.

Gallagher, D. L., and D. A. Gurnett, Auroral kilometric radiation: Time-averaged source position, *J. Geophys. Res.*, *84*, 6501, 1979.

Green, J. L., D. A. Gurnett, and R. A. Hoffman, A correlation between auroral kilometric radiation and inverted-V electron precipitation, *J. Geophys. Res.*, *84*, 5216, 1979.

Gregory, P. C., Radio emission from auroral electrons, *Nature*, *221*, 351, 1969.

Gurnett, D. A., A satellite study of VLF hiss, *J. Geophys. Res.*, *71*, 5599, 1966.

Gurnett, D. A., The earth as a radio source: Terrestrial kilometric radiation, *J. Geophys. Res.*, *79*, 4227, 1974.

Gurnett, D. A., and L. A. Frank, VLF hiss and related plasma observations in the polar magnetosphere, *J. Geophys. Res.*, *77*, 172, 1972.

Gurnett, D. A., and L. A. Frank, Plasma waves in the polar cusp: Observations from Hawkeye 1, *J. Geophys. Res.*, *83*, 1447, 1978.

Gurnett, D. A., and J. L. Green, On the polarization and origin of auroral kilometric radiation, *J. Geophys. Res.*, *83*, 689, 1978.

Gurnett, D. A., and R. R. Shaw, Electromagnetic radiation trapped in the magnetosphere above the plasma frequency, *J. Geophys. Res.*, *78*, 8136, 1973.

Hartz, T. R., Radio noise levels within and above the ionosphere, *Proc. IEEE*, *57*, 1024, 1969.

Hoffman, R. A., and E. R. Schmerling, Dynamics Explorer program: An overview, *Space Sci. Instrum.*, *5*, 345, 1981.

James, H. G., VLF saucers, *J. Geophys. Res.*, *81*, 501, 1976.

James, H. G., Wave propagation experiments at medium frequencies between two ionospheric satellites, 1, General results, *Radio Sci.*, *13*, 531, 1978.

James, H. G., Wave propagation experiments at medium frequencies between two ionospheric satellites, 3, Z mode pulses, *J. Geophys. Res.*, *84*, 499, 1979.

Jones, D., Source of terrestrial non-thermal radiation, *Nature*, *260*, 686, 1976.

Jones, D., Mode-coupling of Z-mode waves as a source of terrestrial kilometric and Jovian decametric radiation, *Astron. Astrophys.*, *55*, 245, 1977.

Jorgensen, T. S., Interpretation of auroral hiss measured on OGO 2 and at Byrd Station in terms of incoherent Cerenkov radiation, *J. Geophys. Res.*, *73*, 1055, 1968.

Kaiser, M. L., and R. G. Stone, Earth as an intense planetary radio source: Similarities to Jupiter and Saturn, *Science*, *189*, 285, 1975.

Kaiser, M. L., J. K. Alexander, A. C. Riddle, J. B. Pearce, and J. W. Warwick, Direct measurements of the polarization of terrestrial kilometric radiation from Voyagers 1 and 2, *Geophys. Res. Lett.*, *5*, 857, 1978.

Kaufman, R. L., P. B. Dunsenbery, and B. J. Thomas, Stability of the auroral plasma: Parallel and perpendicular propagation of electrostatic waves, *J. Geophys. Res.*, *83*, 5663, 1978.

Kennel, C. F., F. L. Scarf, R. W. Fredricks, J. H. McGehee, and F. V. Coroniti, VLF electric field observations in the magnetosphere, *J. Geophys. Res.*, *75*, 6136, 1970.

Kurth, W. S., M. M. Baumback, and D. A. Gurnett, Direction-finding measurements of auroral kilometric radiation, *J. Geophys. Res.*, *80*, 2764, 1975.

Laaspere, T., and R. A. Hoffman, New results on the correlation between low-energy electrons and auroral hiss, *J. Geophys. Res.*, *81*, 524, 1976.

Maggs, J. E., Coherent generation of VLF hiss, *J.Geophys. Res.*, *81*, 1707, 1976.

Maggs, J. E., and W. Lotko, Altitude dependent model of the auroral beam and beam-generated electrostatic noise, *J. Geophys. Res.*, *86*, 3439, 1981.

Martin, L. H., R. A. Helliwell, and K. R. Marks, Association between aurorae and very-low-frequency hiss observed at Byrd Station, Antarctica, *Nature*, *187*, 751, 1960.

Mosier, S. R., and D. A. Gurnett, VLF measurements of the Poynting flux along the geomagnetic field with the Injun 5 satellites, *J. Geophys. Res.*, *74*, 5675, 1969.

Mosier, S. R., M. L. Kaiser, and L. W. Brown, Observations of noise bands associated with the upper hybrid resonance by the IMP 6 radio astronomy experiment, *J. Geophys. Res.*, *78*, 1683, 1973.

Muldrew, D. B., Preliminary results of ISIS 1 concerning electron-density variations, ionospheric resonances and Cerenkov radiation, *Space Res.*, *10*, 786, 1970.

Oya, H., and A. Morioka, Observational evidences of Z mode waves as the origin of auroral kilometric radiation based on AKR data detected by JIKIKEN (EXOS B) satellite, submitted to *J. Geophys. Res.*, 1982.

Poeverlein, H., Strahwege von Radiowellen in der Ionosphäre, *Z. Angew. Phys.*, *1*, 517, 1949.

Ratcliffe, J. A., *The Magneto-Ionic Theory and Its Applications to the Ionosphere*, Cambridge University Press, New York, 1959.

Roux, A., and R. Pellat, Coherent generation of the auroral kilometric

radiation by nonlinear beatings between electrostatic waves, *J. Geophys. Res.*, *84*, 5189, 1979.

Shaw, R. R., and D. A. Gurnett, Electrostatic noise bands associated with the electron gyrofrequency and plasma frequency in the outer magnetosphere, *J. Geophys. Res.*, *80*, 4259, 1975.

Shawhan, S. D., Magnetospheric plasma waves, in *Solar System Plasma Physics*, vol. III, edited by L. J. Lanzerotti, C. F. Kennel, and E. N. Parker, North-Holland, Amsterdam, 1979.

Shawhan, S. D., and D. A. Gurnett, Polarization measurements of auroral kilometric radiation by Dynamics Explorer 1, *Geophys. Res. Lett.*, *9*, 913, 1982.

Shawhan, S. D., D. A. Gurnett, D. L. Odem, R. A. Helliwell, and C. G. Park, The plasma wave and quasi-static electric field instrument (PWI) for Dynamics Explorer-A, *Space Sci. Instrum.*, *5*, 535, 1982.

Smith, R. L., VLF observations of auroral beams as sources of a class of emission, *Nature*, *224*, 351, 1969.

Stix, T. H., *The Theory of Plasma Waves*, McGraw-Hill, New York, 1962.

Storey, L. R. P., An investigation of whistling atmospherics, *Philos. Trans. R. Soc. London Ser. A*, *246*, 113, 1953.

Taylor, W. W. L., and S. D. Shawhan, A test of incoherent Cerenkiov radiation for VLF hiss and other magnetospheric emissions, *J. Geophys. Res.*, *79*, 105, 1974.

Walsh, D., T. F. Haddock, and H. F. Schulte, Cosmic radio intensities at 1.225 and 2.0 MC measured up to an altitude of 1700 km, *Space Res.*, *4*, 935, 1964.

(Received April 8, 1982;
revised September 22, 1982;
accepted October 1, 1982.)